Geometry Optimization of DC and SRF Guns to Maximize Beam Brightness

M.N. Lakshmanan and I.V. Bazarov, CLASSE, Cornell University, Ithaca, NY 14853, USA
T. Miyajima, Photon Factory, KEK, Tsukuba, Japan

Abstract

A set of geometries for DC and SRF guns is studied from the perspective of beam dynamics. The geometries are parameterized and are made a part of an optimization process that minimizes emittance downstream of the gun following the emittance compensation solenoid. The setups simulated are kept to realistic field strengths by imposing an empirical gun voltage breakdown law in the DC gun case and a maximum achievable surface magnetic field for the SRF gun case.

INTRODUCTION

To realize their fullest potential for a range of applications, Energy Recovery Linacs require high brightness high current electron sources operating beyond the state of the art. Photoemission guns, operating with either DC or continuous duty RF fields, are the technology of choice. Very high accelerating gradients at the photocathodes are required to counteract the space charge forces acting on the electron bunches. In DC guns, the strength of the field is typically limited by the field emission and related high voltage breakdown phenomena. Superconducting RF (SRF) guns have the potential to overcome the limitations imposed on DC guns and allow higher operating gradients. The highest accelerating field that can be supported in an SRF gun is limited by the highest (critical) magnetic field on the cavity surface which leads to cavity quenching, even though other practical causes (e.g. field emission) may limit the gradient to much lower values. To transport the space charge dominated beam from the gun to an energy boosting linac, a high gun voltage is also desirable. In addition to high longitudinal accelerating field, field components leading to transverse focusing in the gun are important to ensure proper beam matching and high degree of emittance compensation.

Overall, the gun design is subject to a number of conflicting requirements. For a example, a stronger transverse focusing in DC guns via cathode electrode shaping typically reduces the available accelerating field otherwise possible for the same cathode-anode separation and gun voltage. Similarly, empirical data on voltage breakdown for large area in-vacuum electrodes suggests that much higher gradients are possible at the expense of a shorter gap between the electrodes and the correspondingly reduced gun voltage. Time-varying nature of fields in SRF guns introduces additional complications: the optimal phase of laser pulse arrival can be chosen either to maximize the accelerating gradient at the photocathode, the beam energy at the exit of the gun, or by requiring that the transverse momentum imparted to off-axis particles in the gun nearly does not depend on the position of particles inside the bunch [1]. All these considerations in turn are a function of the gun geometry making it a critical factor in determining the quality of the beams produced.

We have developed a technique to optimize the gun geometries using multi-objective genetic algorithms, which minimizes the beam emittance possible out of the gun while subject to a number of realistic constraints limiting the maximum fields in the gun. We outline our method, provide details on the parameterized gun geometries used in the study, and present the results of computer optimizations for low emittance beams possible from a short beamline that uses DC and (S)RF optimized gun geometries followed by an emittance compensation solenoid and a $\sim 1\text{m}$ drift.

METHOD DESCRIPTION

Parallel genetic algorithm

We have used a multiobjective evolutionary algorithm run on 160 2 GHz parallel processors to extensively survey the multivariate space for optimum solutions [2]. A detailed list of variable parameters (also known as decision variables) is given in Table 1. Refer to [2] and references therein for the description of inner workings of these algorithms. A brief summary follows for the convenience of the unfamiliar reader. The algorithm begins by running a trial set of solutions. Then the "fittest" solutions are selected from the set based on typically two criteria: beam emittance and the gun voltage or gradient. The optimizer seeks to minimize both objective parameters to produce a high brightness beam using a lower voltage in the gun (i.e. finds the smallest emittance possible at any given gun voltage). To form a new trial set for the next "generation", the algorithm applies two operators to the selected solutions of the previous generation: (1) "crossing" or "mating" of two or more solutions; and (2) slightly perturbing ("mutating") each solution to form new solutions ("offspring"). The process is then repeated with the new trial set and continues for a number of generations, effectively exploring the decision variable space for the best solutions. In the process, the solutions are subject to a set of constraints to ensure physically realistic scenarios. Finally, a set of optimal solutions is presented as the optimal front, the so-called "non-dominated set" or "Pareto front".

Treatment of field maps

Through parameterizations, the gun geometry is made a part of the decision variable space to be explored by

ERL09 WG1 SUMMARY: DC GUN TECHNOLOGICAL CHALLENGES

N. Nishimori[1], I. Bazarov[2], B. Dunham[2], J. Grames[3], C. Hernandez-Garcia[3],

L. Jones[4], B. Militsyn[4], M. Poelker[3], K. Surles-Law[3], M. Yamamoto[5]

[1] JAEA, Tokai-mura, Ibaraki 319-1195, Japan

[2] Cornell University, Ithaca, NY 14853, U.S.A.

[3] Jefferson Lab., Newport News, VA 23606, U.S.A.

[4] STFC Daresbury Lab., Warrington, WA4 4AD, U.K.

[5] KEK, Tsukuba, Ibaraki 305-0801, Japan

Abstract

This paper summarizes technological challenges of photoemission DC guns being developed for the future energy recovery linac (ERL) light sources (LS). Anticipated new applications of ERL-LS demand an electron gun capable of producing an extremely low emittance beam at very high average current. The low emittance requires unprecedentedly high voltage equal to or greater than 500 kV between cathode/anode electrodes together with high accelerating gradient on the photocathode. The technological challenge is to develop a high voltage insulator system, which can withstand field emission from the electrodes. A high voltage processing technique and a challenge to suppress field emission are discussed. The high average current requires prolonged cathode life time, which is governed by ion back-bombardment. Challenges to mitigate the cathode damage caused by ion back-bompardment are surveyed. We also discuss high voltage power supply which can afford sufficient high average current, load-lock system capable of accomodating quick cathode exchange to minimize accelerator down time, and vacum technology to suppress both field emission and ion back-bombardment. A gun geometry satisfying both high gun voltage and high accelerating gradient is also proposed.

INTRODUCTION

Electron guns capable of providing reliable CW beam with average current ~100mA and emittance of a few microns (normalized RMS) are being developed for the next generation energy recovery linacs (ERL) light sources in various research laboratories [1,2]. A DC photoemission electron gun with an activated GaAs photocathode illuminated with 532 nm laser light is considered to be one of most promising candidates of the guns for the ERL light sources, since a 350 kV DC gun successfully delivered 9.1 mA CW electron beam to the Jefferson Lab (JLab) 10 kW IR upgrade Free Electron Laser (FEL) [3]. In this paper we survey technological challenges and related developments in DC photoemission electron guns as high current sources for ERLs.

The high voltage power supply determines limits of the maximum beam energy and current from the guns. The low emittance necessary for ERLs typically requires a DC voltage equal to or greater than 500 kV to reduce non-linear space charge effects in the low energy regime [4]. The fluctuation of beam arrival time at insertion devices should be suppressed for pump-probe experiments using fs x-rays from ERLs. A study shows synchronization stability of ERL systems is governed by injector stability [5]. This sets the requirement on the ripple of DC gun high voltage to be on the order of 10^{-3}. The next generation ERL light sources usually require the beam current from 10 mA to 100 mA. Consequently, a high voltage power supply with voltage greater than 500 kV, and stability of 10^{-3} or better and current greater than 10 mA needs to be developed. Conventional Cockcroft Walton high voltage power supplies with voltage above 500 kV and currents up to 10 mA are used in JLab, Daresbury Laboratory (DL), and JAEA/KEK. A high voltage power supply of 100 mA and 750 kV for Cornell Univ. is developed using cross transformer technology [6].

The ceramic insulator is a simple structure to support a cathode electrode inside the vacuum and is electrically connected to a high voltage power supply outside the vacuum. Operation of photoemission guns at voltages greater than 350 kV is however very difficult, since field emission from electrode structures can lead to voltage breakdown, insulator punch-through, and other problems on the ceramics. Recently three ways to resolve the field emission problem have been proposed. The first is the use of a ceramic insulator with a controlled bulk resistivity utilized at DL. This permits any charge build-up on the ceramic surface to be dissipated to ground. Using this insulator technology, 485 kV was achieved during conditioning at DL. The second is an inverted insulator similar to the metal-ceramic X-ray tubes where a high voltage feed passing through the insulator center is connected to a high voltage terminal. The inverted insulator eliminates the electrode structures typical for normal insulators, which might be the sources of field emission. The third is a segmented insulator, where a number of ceramics are stacked in series with Kovar ring electrode sandwiched between adjacent two ceramics. These insulators are widely used in electrostatic

ERL 2009 WG1 SUMMARY PAPER: DRIVE LASERS AND RF GUN OPERATION AND CHALLENGES*

J.W. Lewellen[1], H. Bluem[2], A. Burrill[3], T.L. Grimm[4], T. Kamps[5], R. Legg[6], K. Liu[7], T. Rao[3], J. Smedley[3], J. Teichert[8], S. Zhang[9]

[1] Naval Postgraduate School, Monterey, CA 93943, USA
[2] Advanced Energy Systems, Inc., Princeton, NJ 08824, USA
[3] Brookhaven National Laboratory, Upton, NY 11973, USA
[4] Niowave, Inc., Lansing, MI 48906, USA
[5] Helmholtz-Zentrum Berlin, 14109 Berlin, Germany
[6] University of Wisconsin-Madison, Stoughton, WI 53589, USA
[7] Peking University, Beijing 100871, People's Republic of China
[8] Forschungszentrum Dresden-Rossendorf, 01314 Dresden, Germany
[9] Thomas Jefferson National Accelerator Facility, Newport News, VA 23606, USA

Abstract

Working Group I of the 2009 Energy Recovery Linac Workshop focused on high-brightness, high-power electron beam sources for energy recovery linacs (ERLs), and relevant technology such as development of drive lasers. The WG1 summary paper was broken into two parts: DC guns and loadlocks; and RF guns and drive lasers. This was done both to retain more manageable paper sizes, and because SRF guns are in an earlier stage of development than DC guns. This paper describes the advances, concepts, and thoughts for the latter topics presented at the workshop.

There are many challenges to the successful operation of SRF guns as high-brightness, high-average-current beam sources. These combine the set of challenges for high-current SRF cavities (fabrication, cleaning and processing, HOM extraction, etc.), with challenges for high-average-current photocathode sources (photocathode fabrication, quantum efficiency and lifetime, drive laser technology, etc.). New challenges also arise from this combination, such as the requirement for having removable cathodes in an SRF cavity.   Practical approaches have been, and are currently being, found to address the problems, and the base of knowledge and experience continues to grow.

Alternate ideas are also beginning to make inroads. Hybrid DC-SRF guns, pioneered by Peking University, offer promise for combining the best features of both technologies. Quarter-wave SRF cavities offer compact size for a given frequency, potentially easier fabrication than elliptical cells, and very high transit-time factors for quasi-DC operation. Also, the use of normal-conducting cavities, usually dismissed out of hand due to the required RF power consumption, may become practical with advanced cavity designs.

This paper summarizes the state-of-the-art of drive lasers, cathode development and RF gun-based injectors for ERL beam sources The focus in the field has been on DC and SRF guns to date, but interesting approaches for hybrid DC/SRF guns and normal-conducting RF guns are also presented. The paper concludes with discussions of operational issues and concerns, technical issues related to beam source realization, and future concepts.

SUMMARY ON ERL DRIVE LASERS

S. Zhang and T. Rao

CURRENT STATUS

Significant progress on ERL drive lasers has been seen since ERL07. The status of each drive laser is summarized below based on the reports given by different labs during this workshop (specification details are given in Table 1):

- JLab has replaced its flashlamp-pumped drive laser and commissioned a 25W/532nm diode-pumped MOPA system in 2008. The new drive laser has been driving the JLab ERL FEL with adjustable CW micro-pulse frequency from 75MHz down to below 0.5MHz. The macro-pulse width and frequency are also adjustable up to 1ms/60Hz (limited to 1kHz) for routine machine setup. The system shows better amplitude and temporal stability. Unexpected high degree of phase sensitivity from laser oscillator was observed and still remains a primary concern, although considerable effort has been made to suppress the phase noise. A pulse stacker was also installed to change the laser pulse length and shape [1].

- Daresbury Laboratory's 5W/532nm drive laser was commissioned in 2006 and is running for ERL machine beam operation. The laser system has a 0.2% duty cycle with a fixed 81.25MHz micro-pulse frequency and up to 100us/20Hz macro-pulse structure. An issue of temperature instability has arisen from corrosion inside the cooling circuit. This has caused problems in maintaining the pump diode temperature correctly and stably, resulting in longer pulses and reduced SHG efficiency [2].

STATUS OF THE JEFFERSON LAB ERL FEL DC PHOTOEMISSION GUN

C. Hernandez-Garcia*, S. V. Benson, G. Biallas, J. Boyce, D. Bullard, J. Coleman, D. Douglas, P. Evtushenko, C. Gould, A. Grippo, J. Gubeli, F. Hannon, D. Hardy, M. Kelley, J. Kortze, K. Jordan, J. M. Klopf, M. Marchlik, W. Moore, G. R. Neil, T. Powers, D. Sexton, M. Shinn, C. Tennant, R. Walker, G. Williams, and S. Zhang, TJNAF, Newport News, VA 23606, USA

Abstract

The Jefferson Lab (JLab) Energy Recovery Linac 10 kW IR Upgrade Free Electron Laser (FEL) is driven by a 350kV DC un-polarized photoemission electron gun. In 2003, an upgrade version of the earlier 1 kW IR Demo FEL gun delivered over 1000 Coulombs with a single Cs:GaAs wafer in one year of operation. Between 2004 and 2007 a second wafer delivered over 7000 Coulombs and up to 9 mA CW beam for FEL operations. Both wafers suffered surface damage with total loss of quantum efficiency in several occasions during high current operations. Since then, the electron gun has been refurbished two times after suffering damage caused by excessive field emission. Although presently operating at nominal 350kV, field emission has significantly decreased the photocathode lifetime.

INTRODUCTION

The JLab 10 kW IR Upgrade FEL DC photoemission gun has been in operation since 2003 [1]. The Upgrade Gun operates at 350kV and it is a direct evolution of the earlier JLab 1 kW Demo IR FEL gun that operated at 320kV [2].

The photocathode is 3.2 cm diameter single crystal bulk GaAs wafer, 600 micron thick and Zn-doped at $\sim 1 \times 10^{18}$ cm^{-3}. By retracting it inside the ball electrode, the wafer is activated in-situ into a Negative Electron Affinity (NEA) photocathode. It is illuminated with a frequency-doubled, mode-locked Nd:YLF drive laser to generate 135 pC per bunch. Each laser pulse is 50 ps FWHM at 527 nm. With a repetition rate of 75 MHz the gun delivers electron beam at 10 mA CW [1,2].

In 2003 a bulk GaAs wafer from Matek delivered over 1000 Coulombs and up to 9 mA CW. In 2004 it was replaced with a second wafer from AXT and was in service for three years, until a leak in the gun vacuum chamber opened while operating the gun at 400 kV. A field emitter developed on the support electrode even though the gun had been conditioned up to 450kV in 2004 and operated at 350kV for thousands of hours. Failure of the Machine Protection System to shut down the high voltage power supply led to a catastrophic leak when 100 μA of field emission current heated the 14-inch conflat flange Cu gasket and SF^6 leaked into the vacuum chamber.

In early 2008 the gun was rebuilt with a third wafer. During the high voltage-conditioning phase, one of the ceramic insulators suffered a puncture from excessive field emission. The insulator and the support tube electrode were replaced, the gun was re-built and in the fall of 2008 it was high-voltage conditioned again without much success, until processing with Krypton gas [3]. However, excessive field emission from the wafer prevented FEL operations. In January 2009 a new wafer was installed, and the gun had to be re-conditioned with Kr gas processing. Although the field emission, identified to be from the ball cathode, is on the order of a few micro-Amperes at 350kV, the gas desorption induced by field emitted electrons striking the chamber is sufficient to decrease the photocathode lifetime from 50 operational hours observed in 2004-2007, to only 8 operational hours. The implementation of a motorized cathode manipulator system has reduced FEL down time for quantum efficiency replenishing (re-cesiation) from 3.5 hours to 0.5 hours.

PHOTOCATHODE PERFORMANCE

The Matek GaAs wafer installed in May 2003 delivered over 1000 Coulombs in one year of service and up to 9 mA CW beam (122pC per bunch at 350 keV) [1]. The second wafer, from AXT, was anodized around the edge leaving a 1.6 cm diameter active area to reduce electron beam halo caused by drive laser scatter light. The drive laser spot on the cathode was kept at 0.8 cm diameter and at 0.4 cm off the electrostatic center to avoid the Quantum Efficiency (QE) degradation spot by back-ion bombardment. This wafer was in service for 36 months and was activated into a NEA photocathode 9 times achieving routinely 6-7% QE. The QE was replenished six times between activations by spraying fresh Cesium onto the photocathode surface. If the photocathode were re-cesiated more than six times, Cesium would accumulate on the surface leading to tens of nano-Amperes of field emission observed on a phosphor screen beam viewer downstream of the gun. Typically 96% of the previous QE was recovered with each re-cesiation. The 1/e lifetime was 550 Coulombs or 50 operational hours with 5 mA CW beam (135pC per bunch at 350 keV). The total extracted charge from that wafer was 7000 Coulombs in 900 operational hours with a beam current between 1 and 8.5 mA CW.

Both wafers, the Matek and the AXT, suffered surface damage while delivering beam in excess of 8.5 mA CW for FEL operations. Beyond that current level, the injector SRF booster suddenly tripped off on waveguide vacuum fault and the pressure in the gun vacuum chamber raised

3D LASER PULSE SHAPIG, MEASUREMENT, AND 3D ELECTRON BEAM PROFILE MEASUREMNT FOR PHOTOINJECTORS

Yuelin Li, ANL, Argonne, IL 60439, U.S.A.

Abstract

We propose a scheme of shaping laser pulses in 3D exploiting chromatic aberration and laser phase tailoring. We demonstrated an interferometry method of measuring 3D distribution of a laser pulse. For the electron beam diagnostics, a non interceptive time resolved laser wire scheme is proposed using a ultrafast laser pulse in a line focus to scatter from the beam under consideration. By imaging the scattered photons at different delays between the laser and the beam, the 3D distribution can be reconstructed.

INTRUDCUTION

For high brightness photoinjectors, it is critical to be able to shape the 3D form of the drive laser pulse, to understand its actual 3D distribution, and the initial electron beam in order to properly compensate the emittance growth [1, 2].

We propose a 3D pulse shaping scheme which can be potentially used to generate 3D uniform ellipsoidal beam [3]. In a proof of principle experiment [4, 5], we demonstrated that the shaping method and at the same time developed a method for measuring the 3D distribution of a laser pulse based on a crossing interferometer. We also propose to use a time-resolved laser wire to measure the 3D distribution of a low energy electron beam, e.g., one that is leaving a photoinjector, based on imaging the photons scattered from the electron beam from a ultrafast laser pulse.

3D LASER PULSE SHAPING

To shape the laser pulse in 3D, we exploit the chromatic aberration effect in an optical lens. The dependence of the refractive index upon the optical frequency gives rise to the chromatic aberration in a lens, where the change of the focal length due to a shift in frequency $\delta\omega$ is

$$\delta f = -\frac{f_0}{n_0-1}\chi\delta\omega, \qquad (1)$$

where f_0 is the nominal focal length at ω_0. We assume a constant $\chi = dn/d\omega$ for this analysis. For a Gaussian beam, the beam size at the nominal focal plane is

$$w \approx w_0\left[1+\left(\delta f/z_R\right)^2\right]^{1/2}. \qquad (2)$$

Here $w_0 = N\lambda_0/\pi$ is the beam waist at the nominal wavelength λ_0, with N the numerical aperture, and $z_R = \pi w_0^2/\lambda_0$ is the Rayleigh range. It is obvious, therefore, if one can program $\delta\omega$ in time, a time-dependent beam size can be achieved. At $\delta f \gg z_R$, one has $w(t) \cong |\delta f(t)|/N$,

thus the phase of the laser pulse is

$$\phi(t) = \pm\int\delta\omega(t)dt = \pm\frac{n_0-1}{\chi}\frac{N}{f_0}\int w(t)dt \cdot \qquad (3)$$

For a desired time-dependent intensity $I(t)$, the amplitude of the laser should be

$$A(t) \propto I(t)^{1/2}w(t) \cdot \qquad (4)$$

As an example, to generate an ellipsoidal radial envelop with maximum radius of R and full length of $2T$, the transverse beam size as a function of time is $w(t) = R[1-(t/T)^2]^{1/2}$. Using Eq. (3), this in turn gives the phase,

$$\phi(t) = -\omega_0 t \pm \frac{\Delta\omega}{2}\left[t\left(1-\left(\frac{t}{T}\right)^2\right)^\alpha + T\sin^{-1}\frac{t}{T}\right], \qquad (5)$$

where $\alpha = 1/2$, and $\Delta\omega = (n_0-1)NR/\chi f_0$ is the maximum frequency shift. To keep the laser flux $|A(t)|^2/w(t)^2$ constant over time, we have

$$A(t) = A_0\left[1-\left(\frac{t}{T}\right)^2\right]^\eta, \qquad (6)$$

with $\eta = 1/2$. Equations (4) and (5) describe a pulse that can form a spatiotemporal ellipsoid at the focus of the a lens. In particle tracking simulations, the performed of so generated ellipsoidal beam give excellent emittance performance [3, 5].

3D LASER PULSE MEASURMENT

Method

The scheme is based on the interference between the drive laser pulse and a short interrogation pulse. The schematic of the experiment is shown in Fig. 1. Assuming that the interrogation (probing) laser and the main laser pulse has a field distribution as $A_{p,m}(t, \boldsymbol{r})$, the interference pattern on the detector is:

$$I(\boldsymbol{r}) = I_m(\boldsymbol{r}) + I_p(\boldsymbol{r}) + 2\cos(\omega[\tau+\delta(\boldsymbol{r})])\times$$
$$\int A_m(t,\boldsymbol{r})A_p(t-\delta(\boldsymbol{r})-\tau,\boldsymbol{r})\cos[\phi_m(t)-\phi_p(t-\delta(\boldsymbol{r})-\tau)]dt, \qquad (7)$$

where

$$I(\boldsymbol{r}) = \int|A(t,\boldsymbol{r})|^2 dt, \qquad (8)$$

is the integrated intensity and $\phi(t)$ is the phase of the laser beams; the subscripts m and p denote the main and probe beam, respectively; τ is the timing delay and $\delta(\boldsymbol{r})$ is the additional location dependent delay due to the angle between the two beams, respectively. The phase term in the integral, though impossible to evaluate for each location, only causes the interference fringes at the detector to shift. Therefore, if the probe pulse is much shorter than the main pulse, Eq. (7) can be reduced to

SRF PHOTOINJECTOR R&D AT UNIVERSITY OF WISCONSIN*

R. Legg[#], M. Allen, M. Fisher, A. Hjortland, K. Kleman, University of Wisconsin, Madison, WI
T. Grimm, M. Pruitt, Niowave Inc., Lansing, MI, U.S.A.

Abstract

Next generation light sources will enable significant new science in the many disciplines including atomic and fundamental physics, condensed matter physics and materials sciences, femtochemistry, biology, and various fields of engineering. The source we propose, and the experimental methods it will spawn, will generally be qualitatively new and have high impact through ultrahigh resolution in the time and frequency domains combined with full transverse coherence for imaging and nanofabrication. Continuous wave FEL's provide the highest beam brightness[1], full temporal and transverse coherence and the potential for ultra short photon pulses at high repetition rates that the science requires. But the hardware, in particular the injector, to build such a light source has not been demonstrated yet. University of Wisconsin, in collaboration with the Naval Postgraduate School, has been engaged in a design contract with Niowave Inc to design a superconducting rf electron gun to be used for such a source. This design work and our collaboration with the Naval Postgraduate School in the construction and test of their SRF gun will allow us to produce a prototype device in a timely and cost effective manner. The design for such a development enables a User facility with the capability to explore the science in the grand challenges laid out by DOE BESAC[2] and the Science and Technology of Future Light Sources white paper[1].

BACKGROUND AND OVERVIEW

The challenges laid out in the DOE BESAC grand challenges in science and energy require new photon sources. Current accelerator technology cannot support the required goals for those sources technically. Additional accelerator research and development is required in order to enable the science in the grand challenges. The University of Wisconsin has proposed a seeded FEL, the Wisconsin Free Electron Laser (WiFEL), which is differentiated from today's synchrotron facilities or laser sources because it combines high power and coherence for the first time in the 1 to 100 nm range. The source we propose, and the experimental methods it will spawn, will generally be qualitatively new and have high impact through ultrahigh resolution in the time and frequency domains combined with full transverse coherence for imaging and nanofabrication.

The key features of the facility we envision are demanded by the scientific mission. A seeded FEL would take advantage of the flexibility, stability, and high average pulse rates available from a continuous-wave (CW) superconducting linac fed by a superconducting photoinjector. For example, a second generation seeded FEL[1] is capable of producing the very bright and short pulses required to produce the science. In order to produce beams of the highest quality, the electron beam will be seeded with high harmonics of laboratory lasers. The required electron beam requirements at the insertion devices for such a device are shown in Table 1.

Table 1: FEL Requirements

I ave, Rf power coupler limited	~ 1 mA
I peak at Undulator	1000 Amps
DI / I at Undulator	10% Max
Normalized ε Transverse	<1 mm-mrad
Bunch length, rms	70 fsec
Charge/bunch (derived)	200 pC
Gun Repetition frequency	Up to 5 MHz

The one milliamp limit for a linac based light source in the table is a function of the coupler limitations of the present generation of high gradient L-band superconducting modules. Both Tesla and Jefferson Lab 100 MeV cryomodules have couplers which can handle about 10 kW of rf power per cavity with about 10 MeV of acceleration per cavity, limiting their current handling to about 1 milliamp without energy recovery. Certain cavities such as the JLAB FEL injector quarter cryomodule and the Cornell eight cell modules can surpass this limitation, but these modules are much larger and more expensive per MeV of acceleration in both procurement and in tunnel footprint required.

The peak current required by the insertion device is about 10^3 amps with the FEL-gain proportional to the electron density in the bunch[3]. Only 10% $\Delta I/I$ modulation on the current waveform is allowed during the interaction between the seed laser and the electron bunch. These modulations produce enhanced spontaneous radiation which competes with the seed laser to modulate the rest of the electron bunch; in the worst case, the spontaneous radiation produced by the charge density fluctuations may destructively interfere with or produce sidebands around the seed laser wavelength. The User community the WiFEL is designed to serve also expect very little variation in optical power just as they would receive from a synchrotron light source. This 10% $\Delta I/I$ limitation is exacerbated by the magnetic bunching chicanes which squeeze the bunches longitudinally after the injector to reach the necessary kiloampere levels in the undulators but can also cause sharp density spikes in the compressed bunch by amplifying existing longitudinal modulations. Gain factors can reach 10^6 for a two chicane system [4], Fig 1. To mitigate this effect, weak compressors are used, increasing the peak current required from the gun.

Injectors, Guns, & Cathodes

LATTICE DESIGN OF 2-LOOP COMPACT ENERGY RECOVERY LINAC

Miho Shimada[1], Yukinori Kobayashi

High Energy Accelerator Research Organization, KEK

1-1 Oho, Tsukuba, Ibaraki, 305-0801

Abstract

Compact Energy Recovery Linac (Compact ERL) is planned to construct in the KEK site as a test facility of 5GeV-ERL project. For achieving the high energy with a limited refrigeration power, the electron beam is accelerated twice by the same super-conducting cavity in a 2-loop design. At the branch of the two loops, a chicane is installed for flexibility of the ratio of the lower energy in the inner loop to higher energy in the outer loop. The angle of merger of the injection is 16 degree. The linear optics of the linear accelerator section is optimized for the two accelerator and two decelerator beams using the "dummy loop", which is used for determination of the twiss parameters of the entrance/exit of the two loops. Both inner and outer loop are designed to be an achromat and isochronous.

1. Introduction

5GeV energy recovery linac project has been promoted as the next generation light source, which is planned to be sited in KEK. For saving the building cost, site area and the refrigerating power, 2-loop scheme is a strong candidate for KEK project as well as others projects, such as Cornell Laboratory [1]. On the other side, the higher order mode (HOM), which accumulated in the superconducting cavity at lower current and the complicated beam dynamics are critical issues.

Compact ERL, which is a test facility of 5GeV-ERL, is using 2-loop scheme for achieving the higher electron energy with a limited refrigerating power. For optimization of the optical functions, the main linac section is should be careful because two accelerating and two decelerating beams pass though the same magnets. In this paper, we proposed the method of optimisation of optical functions and the simulation results for the Compact ERL.

2. Lattice layout of 2-loop Compact ERL

2.1 Main parameters and magnet layout

Figure 1 shows the schematic drawing of the layout of the Compact ERL. 500kV electron beam from DC photo cathode electron gun [2] is accelerated up to 5MeV at the injection section and lead to the main linac section at the merger section, which is composed of three bending magnets [3]. The electron beam accelerated up to 65 MeV passes though the inner loop and then is accelerated again up to 125 MeV. 125 MeV electron beam passing though the outer loop is decelerated twice at the main linac section down to 5 MeV. 5 MeV electron beam is lead to the dump with the extraction section. Total electron path length and the site area of the circulating section are 291.9 m and 47 m × 9.3 m, respectively. The lengths of the two main superconducting cavities are 8m and 10m, which contain four 9 cell-cavities in one cryostat and in two cryostats, respectively [4]. 60MeV acceleration per a turn will be upgrade to 120MeV in the future, in which the maximum electron energy is 245 MeV.
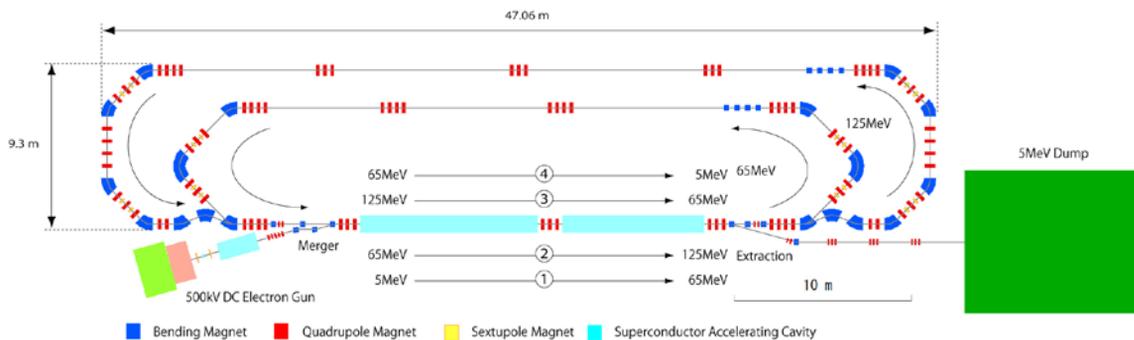

Fig. 1 : Schematic of 2-loop of compact ERL

UNDULATOR OPTIMIZATION FOR ERL BASED LIGHT SOURCES

Robert Rossmanith, Research Center Karlsruhe, Axel Bernhard, Sandra Ehlers, Golo Fuchert, Peter Peiffer, Tilo Baumbach, University Karlsruhe, Germany

Abstract

   Conventional synchrotron light sources operate with currents between 200 and 500 mA. The maximum obtainable brilliance is 10^{21} photons per sec, per 0.1 bandwidth, per mm^2 and per $mrad^2$. In this paper the brilliance of photon beams generated by ERL`s are compared with the brilliance   produced by synchrotron radiation storage rings.

COMPARISON OF THE AVERAGE BRILLIANCE OF ERL BASED LIGHT SOURCES WITH CONVENTIONAL 3RD GENERATION SOURCES

The wavelength λ emitted from a planar undulator is

$$\lambda = \frac{\lambda_u}{2n\gamma^2}(1+\frac{K^2}{2}) \qquad (1)$$

λ_u is the period length of the undulator, γ is the beam energy divided by the electron rest energy, n is 1, 3, 5,…. and K is

$$K = 0.935.\ B[T].\ \lambda_u\ [cm] \qquad (2)$$

B is the maximum magnetic field in Tesla.
   PETRA III is the synchrotron light source with the at the moment highest design brilliance of about 10^{21} photons per sec, per 0.1 bandwidth, per mm^2 and per $mrad^2$ (photon energy circa 10 keV). The minimum gap width of the PETRA III undulators is 9.5 mm, the period length is 23, 31.4 or 29 mm, the total length of one undulator is 2 or 5 m [1]. The design horizontal emittance is 1 nm, the design vertical emittance is 0.01 nm. The total beam current is 100 mA [2].
   In ERL based sources the electron beam is produced in electron guns. In most of the designs the normalized emittance of the gun is both horizontally and vertically identical and in the order of one to several µm. Adiabatic damping reduces the emittances to 0.6 nm at 2.5 GeV and 0.085 nm at 6 GeV when it is assumed that the normalized emittances are 1 µm. Fig. 1 shows the calculated brilliance curve [3] for a 2 m long undulator. The undulator parameters are the same as before for PETRA III: the period length is 23 mm, and the assumed k-value ois 2.2. For a better comparison the current is 100 mA.
   Comparing the values obtained for the model – ERL with the PETRA III parameters fig. 1 clearly shows that for the given parameters the maximum achievable

brilliance in an ERL is somewhat lower than in a storage ring. This is due to the different beam cross- sections In a storage ring the horizontal emittance is significantly higher and the vertical emittance is significantly lower than in an ERL. Only at higher beam energies (6 GeV and higher) the brilliance obtained with an ERL and the brilliance obtained with a storage ring are comparable.
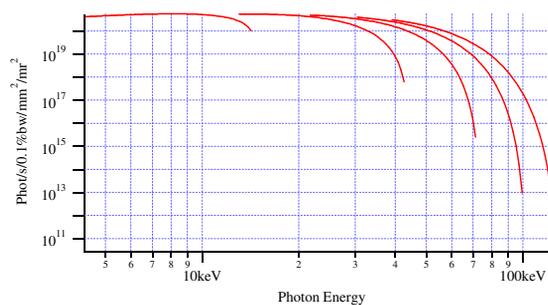

Fig. 1. Calculated brilliance of an ERL based light source. The beam current is 100 mA, the beam energy 6 GeV. The undulator length is 2 m, the period length is 23 mm and k is 2.2. Horizontal and vertical emittance are identical 0.085 nm (normalized emittance 1 µm).

   The brilliance in an ERL versus beam energy is shown in fig. 2. The beam current is 100 mA and the normalized emittance is 3 µm. The undulator parameters from fig. 1 are used. At lower beam energies the beam dimension are larger and limit the brilliance. At very high energies the ERL brilliance would exceed the ERL brilliance.
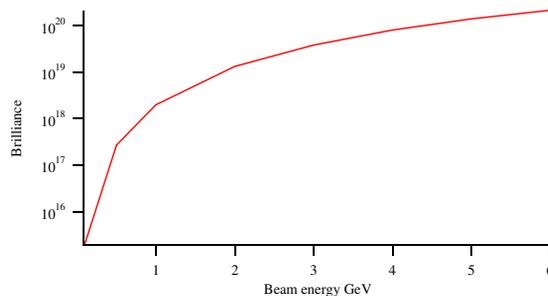

Fig. 2 Brilliance of an ERL for a 100 mA beam (photons per sec, per 0.1 % band width, per mm^2 and per $mrad^2$) . The gun has a normalized emittance of 3 µm, the undulator is 2 m long, the period length is 23 mm and K is 2.2.

Optics & Beam Dynamics

KEK ERL CRYOMODULE DEVELOPMENT

H. Sakai*, T. Furuya, E. Kako, S. Noguchi, M. Sato, S. Sakanaka, T. Shishido, T. Takahashi,
K. Umemori, K. Watanabe and Y. Yamamoto
KEK, 1-1, Oho, Tsukuba, Ibaraki, 305-0801, Japan

M. Sawamura
Japan Atomic Energy Agency (JAEA), Tokai, Naka, Ibaraki 319-1195, Japan

K. Shinoe
Institute for Solid State Physics (ISSP), University of Tokyo, Kashiwa, Chiba 277-8581, Japan

Abstract

Development of a SC Cavity Injector Cryomodule and Main linac Cryomodule for the compact ERL (cERL) [1] is being continued at KEK since 2006. Design of an injector cryomodule containing three 2-cell 1.3-GHz cavities for Injector Cryomodule and two 9-cell 1.3-GHz cavities for Main linac Cryomodule are almost completed. Status of R&D and design details are reported.

INJECTOR FOR CERL

An injector for cERL is required to accelerate a CW electron beam of 100mA to 10MeV. In this application, critical hardware components are not cavities but RF input couplers and HOM dampers. Several combinations of number of cavity and cells per cavity were examined, and a three 2-cell cavity system was chosen for cERL. Each cavity is drove by two input couplers to reduce required power handling capacity and also to compensate coupler kick. HOM coupler scheme was chosen for HOM damping, and 5 HOM couplers are put on beam pipes of each cavity. Because of simplicity cavities are cooled by jacket scheme. Basic parameters of the cavity are summarized in Table 1.

Table 1: Basic Cavity Parameters of injector

Frequency	1.3	GHz
Number of cell	2	
R / Q	205	Ω
Operating Gradient	14.5	MV / m
Number of Input Coupler	2	
Coupler Power	167	kW
Coupler Coupling Q	3.3×10^5	
Number of HOM coupler	5	
Operating Temperature	2	k

cavity

A 2-cell cavity is shown in Figure 1. It has a TESLA-like cell shape and larger beam pipe aperture of 88mm. Two fully equipped prototype cavities were fabricated, and the first cold test in a vertical cryostat was done in the last March. The cavity gradient reached 30MV/m with small electron loading (Figure 2). The reason of low Q value is due to losses at beam pipe flanges made of

* sakai.hiroshi@kek.jp

stainless steel. During the test, we observed some thermal instability (blue dots in Fig. 2), where both Q and gradient decrease slowly. It is well known due to the heating of pick-up antennae of HOM couplers. Heating of one HOM coupler was detected by thermometer at around 16 MV/m, but finally we could keep 16 MV/m for 6 hours.
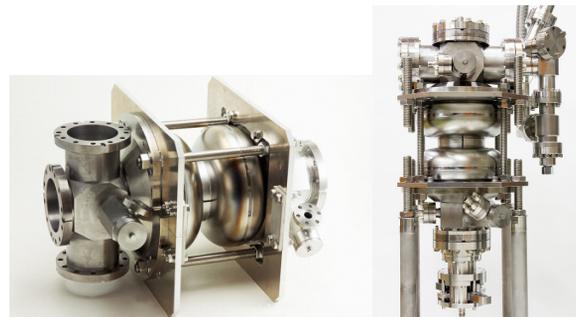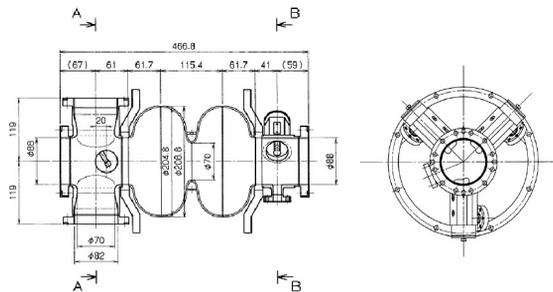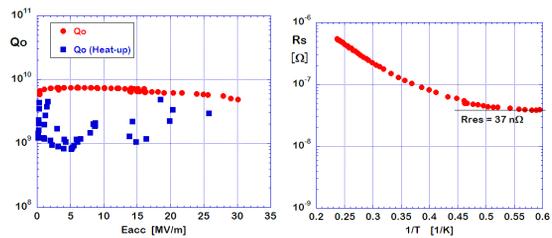

Figure 1: 2-cell Cavity

Figure 2: Vertical Test Results.

Input Coupler

RF input coupler is the most critical component in the high power application of the superconducting cavity. The most powerful CW coupler under operation is the KEK-B couplers, which has a coaxial disk type window

ERL HOM ABSORBER DEVELOPMENT IN JAPAN

M. Sawamura [#], JAEA, Tokai, Ibaraki, Japan
T. Furuya, H. Sakai, K. Umemori, KEK, Tsukuba, Ibaraki, Japan
K. Shinoe, ISSP, Univ. of Tokyo, Kashiwa, Chiba, Japan

Abstract

A superconducting main cavity for ERL has been designed and fabricated to reduce the HOM problem for the high current operation [1]. HOM power propagating along the beam pipe is damped at a HOM absorber installed between the cavities. The HOM absorber is cooled down to liquid nitrogen temperature in a cryo-module. The RF absorber material used for the HOM absorber is required to have good frequency and temperature properties. The frequency and temperature dependences of permittivity and permeability are measured for some ferrites and ceramics with a cold test stand consisting of a GM refrigerator. The parameters of the HOM absorber such as length, thickness and position are optimized by calculation of microwave simulation codes. Test models of the HOM absorber are being designed and fabricated to test the RF, mechanical, cooling and temperature properties.

PROPERTIES OF RF ABSORBER MATERIAL

Frequency and temperature properties of permittivity and permeability for several RF absorber materials were measured. Nicolson-Ross method [2] was used to measure the permittivity and permeability. The procedure of this method is followings.

1) Manufacture material samples to a coaxial shape to set in the 7mm-connector type sample holder.
2) Measure s-parameters of reflection and transmission for the sample with a network analyzer.
3) Calculate the complex permittivity and permeability from the reflection and transmission coefficients.

The samples must be cooled to measure the temperature property. A cold test stand with a GM refrigerator was used to cool the samples from room temperature to 40 K. This cold test stand consists of a GM refrigerator, a compressor, a vacuum chamber, a vacuum pump, and a temperature controller as shown in Fig.1. The GM refrigerator adiabatically expands the helium gas by a piston motion of a displacer. The compressor supplies the compressed helium gas to the GM refrigerator. The vacuum chamber prevents the sample from ice-up due to cooling with the GM refrigerator. The vacuum pump evacuates the air in the vacuum chamber. The temperature controller keeps the sample temperature constant

Figure 2 shows the inside of the vacuum chamber. The cold stage is connected to the cold head of the GM refrigerator and holds on the sample. The heater cable is winded around the cold stage and the heater power is adjusted to keep the temperature of the cold stage constant. The heater power is controlled by the temperature controller. The resistance-temperature detector measures the temperature of the cold stage and is used for the temperature control.

The cold stage is screened by the cylindrical cover wrapped with a super-insulator to prevent the radiation heat from the vacuum chamber.

Calibration of the network analyzer was done at each temperature of measurement. The procedure of the temperature property measurement is following.

1) Connect the calibration kit to the line from each port of the network analyzer and set on the cold stage..
2) Measure the s-parameters of the temperature dependence by cooling with the cold test stand.
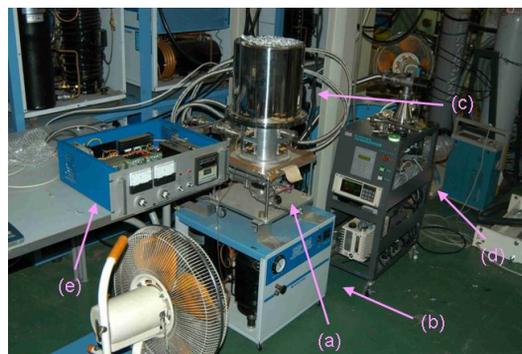

Fig.1 The cold test stand; (a) GM refrigerator, (b) Compressor, (c) Vacuum chamber, (d) Vacuum pump, and (e) Temperature controller.
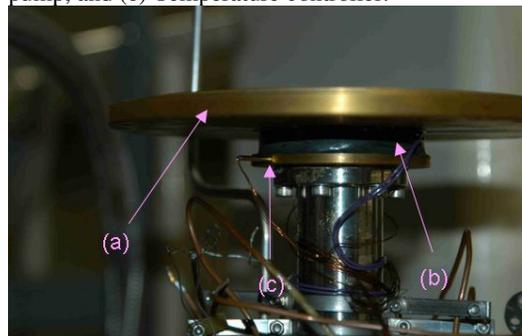

Fig.2 Inside of the vacuum chamber; (a) Cold stage, (b) Heater, and (c) Resistive-temperature detector.

_____
[#]sawamura.masaru@jaea.go.jp

RF & Cryomodules

FAST FERROELECTRIC PHASE SHIFTER DESIGN FOR ERLs *

S.Yu.Kazakov,[a,b] S.V.Shchelkunov,[c] V.P.Yakovlev,[a,d] A.Kanareykin,[e]
E.Nenasheva,[f] J.L.Hirshfield[a,c]

[a]*Omega-p,Inc., 199 Whitney Ave., New Haven, CT 06511, USA*
[b]*High Energy Accelerator Research Organization, KEK, Tsukuba, Ibaraki 305-0801, Japan*
[c]*Beam Physics Laboratory, Yale University, 272 Whitney Avenue, New Haven, CT 06511, USA*
[d]*Fermi National Accelerator Laboratory, Batavia, IL 60510, USA*
[e]*Euclid Concept LLC, Solon, Ohio 44139, USA*
[f]*Ceramics Ltd., St. Petersburg, 194223, Russia*

Abstract

Fast phase shifters are described that use a novel BST ceramic that can rapidly change its dielectric constant as an external bias voltage is changed. These phase shifters promise to reduce by ~10 times the power requirements for the RF-source needed to drive an energy recovery linac (ERL). Such phase shifters will be coupled with SRF cavities so as to tune them to compensate for phase instabilities, whether beam-driven or those caused by microphonics. The most promising design is presented, which was successfully cold-tested and demonstrated a switching speed of ~30 ns for 77 deg, corresponding to <0.5 ns per deg of RF phase. Other crucial issues (losses, phase shift values, etc) are discussed.

INTRODUCTION

In ERLs there are several factors which significantly affect the required wall-plug power. With small beam loading, RF power requirements are determined by Ohmic wall losses, imbalance between beam currents, and microphonics. Compensation for the latter two typically requires a rapid change in coupling between the cavity and feeding line, and attendant high bandwidth, leading to need for significant additional RF power. If beam loading is not small, there are beam-driven phase instabilities for which compensation will also demand additional power.

Compensation can be either by changing the cavity geometry to offset detuning caused by phase instabilities and/or microphonics [1,2], and/or to apply a corrective phase shift to the reflected RF wave that is reintroduced to the cavity so as to cancel phase instabilities [3,4]. The first strategy is accomplished by internal or external motors, or fast internal mechanical piezoelectric tuners. The second approach utilizes fast ferrite or ferroelectric phase shifters that are external to the cryomodules, whereas piezoelectric and other mechanical tuners require operation at cryogenic temperatures and thus permit only limited access in the event of a failure. Further, piezoelectric devices have mechanical resonances which may interfere with control system performance if their own resonance frequency overlaps with the microphonics excitation to be controlled [5]. It is unknown if piezoelectric tuners are efficient enough at high frequencies.

Ferrite phase shifters [6,7,8] are presently limited in their response time to ~30 μs, while the required response time may be only a few μs. The limitation comes mainly from the eddy currents in the ferrite material [7].

Need for μs response time is dictated by the phase and amplitude stability requirements of ~ 0.06 deg and 3e-4, as cited for the Cornell ERL [9]; requirements are similar for the electron cooler project at BNL [10]. The gain in the control feedback loop should be high enough, and its bandwidth wide enough, to insure this high degree of stability. This translates to a bandwidth of about 1 MHz, and rules out contemporary ferrite tuners.

The authors have studied several designs for a fast electrically-controlled ferroelectric phase shifter for ERL applications. The device is to allow changing the RF-coupling during the cavity filling process in order to effect significant power savings, and also to provide rapid compensation for beam imbalance and allow for fast stabilization against phase fluctuations caused by microphonics and beam-driven instabilities. This capability should allow a reduction by about an order-of-magnitude in the required power from the RF source.

POSSIBLE RF POWER SAVINGS

The RF power P_g required to maintain an accelerating voltage V is given by [11]

$$P_g = \frac{V^2(1+\beta)^2}{4\beta Q_0(r/Q)}\left(\left(1+\frac{I_{Re}(r/Q)Q_0}{V(1+\beta)}\right)^2 + \right.$$

$$\left. +\left(\frac{Q_0}{1+\beta}\left(\frac{\omega_0}{\omega}-\frac{\omega}{\omega_0}\right)-\frac{I_{Im}(r/Q)Q_0}{V(1+\beta)}\right)^2\right),$$

where ω_0 is the cavity resonance frequency; Q_0 is it's unloaded quality factor; β is the coupling factor, for SC cavity $\beta \gg 1$; r/Q is the cavity impedance; $I_{Re} = I(\cos\delta\varphi_a - \cos\delta\varphi_d)$, $I_{Im} = I(\sin\delta\varphi_a - \sin\delta\varphi_d)$, $\delta\varphi_a$ and $\delta\varphi_d$, are the average phases of the accelerating and decelerating beams compared with the RF phase; and I is the beam current. The value $\delta\omega = \omega_0 - \omega$ is determined by the amplitude of uncontrolled noise.

In [10,12], an example is given for a cooler linac having two cavities with $Q_0 \approx 4.5\times10^{10}$ at 2°K and $r/Q \approx$ 400 Ohms/cavity, $I = 50mA\times2 = 100$ mA and $V \approx 25$ MV.

RF & Cryomodules

Production of Thermal Positrons at ERL

Alexander Mikhailichenko

Cornell U., Ithaca NY 14853

Abstract. For generation of slow positrons at ERL, we are suggesting the usage of helical ~10T wiggler installed at 5 GeV route for generation of hard gammas. Despite the critical photon energy of radiation is about 170 keV only, the flux in hard part of spectra with photon energy $\hbar\omega > 2mc^2$ generated by 100 mA 5 GeV beam is big enough for generation of polarized thermal positrons with the rate ~10^{11} e^+/sec.

OVERVIEW

ERL oriented generally for generation of electromagnetic radiation (SR/X-rays) for further usage this radiation for investigation in different sciences. One more application of ERL might be in creation of positrons by these radiations and usage of positrons instead of photons may open new possibilities in sciences.

Slow (thermal) positrons are a powerful instrument for investigation of properties of materials [1]-[7] due to their negative affinity to the media. Typically slow positron energy lies within <1 *keV*. Broad usage of positrons for this business slowed down by absence of intense source of low energy positrons with appropriate flux.

What for slow positrons could be used is described well in the references mentioned above. Among them are:

- Transmission and scanning microscopy; mostly promising emerges the possibility to switch between electrons/positrons for better resolution.
- Probing the surface by measuring the energy loss, diffraction and re-emission.
- Defects searching. As positrons could be trapped easily in volume defects even by single missed atom defect, theirs annihilation could be identified by measuring to point of creation of gammas created by annihilation process.
- Probing the Fermi-surface. Pair annihilation and following two-photon emission rate is proportional to the local electron density. The point of creation of two (or rarely three) photons could be resolved with adequate resolution ~nm^3 by measuring Doppler shifts in each photon and deflection from straight line.
- Positron holography.
- Some others, see [1] and references in there.

One way in use for positron creation is a beta decay of isotopes ^{22}Na(2.6 year half life time) or ^{58}Co (71day). The isotopes of ^{64}Cu (12.7 hour), ^{18}F (110 min), ^{11}C(20 min) are in use for these purposes also.

There is basically other practical way for getting the positrons in vast amounts: via electron-positron pair creation by gamma quanta (photon) of appropriate energy and flux in a field of nuclei. The photons in its turn could be generated either by beamstrahlung of electrons in the field of nuclei or by synchrotron or undulator radiation (SR or UR). SR or UR radiation to be effective must create the quantas of appropriate energy $E_\gamma \geq 2mc^2 \cong 1.22\ MeV$. Typically to be

RECENT PROGRESS ON BEAM-BREAKUP CALCULATIONS FOR THE CORNELL X-RAY ERL

J. A. Crittenden, * G.H. Hoffstaetter, M. Liepe, C.E. Mayes, and D.C. Sagan
CLASSE, Cornell University, Ithaca, NY 14853-8001

Abstract

Beam-breakup calculation algorithms have been developed in the general framework of the Cornell X-ray ERL design software, enabling their extension to multi-pass optics design for ERLs. A status report of this work is presented, together with initial results comparing the instability thresholds calculated for single- and two-turn optics with recently developed RF cavity designs.

INTRODUCTION

The potential for excellent quality of X-ray beams from low-emittance electron beams produced by a 5-GeV superconducting energy-recovery linac (ERL) is motivating an extensive development study at Cornell. Figure 1 shows the present status of the design layout on the Cornell campus.
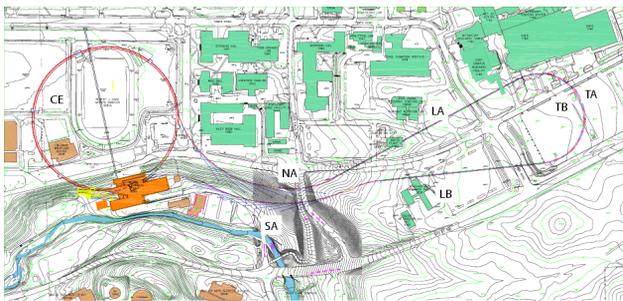

Figure 1: Layout of the Cornell X-ray ERL.

The 10 MeV electron beam produced by the injector is accelerated to 2.8 GeV in the first linac (LA), transported to the second linac (LB) by the high-energy turnaround (TA), where it is accelerated to 5 GeV. The south arc (SA) provides X-ray beamlines, the present CESR ring (CE) is used to transport the beam to the North Arc (NA) beamlines, then the first linac decelerates the 5 GeV beam to 2.2 GeV, and the inner turnaround (TB) transports the beam to the second linac where it is decelerated to 10 MeV and stopped.

Beam-breakup (BBU) instabilities arising from the excitation of higher-order modes in the superconducting RF cavities in the main linacs are important contributions to the operational current limit [1]. The original quantitative estimates of the instability threshold limits in the case of continuous wave recirculators have been extended to energy-

---

* crittenden@cornell.edu

Optics & Beam Dynamics

recovery linacs [5] and generalized to coupled optics and polarized higher-order modes (HOMs) [6]. More recently, detailed numerical estimates for the Cornell one-turn ERL design have been obtained [7]. This paper reports on the implementation of such calculations in Bmad, the lattice analysis and design software package developed at Cornell for the ERL, CESR and other projects [3]. Primary motivation for this work is the extension to multi-pass ERLs.

BEAM-BREAKUP CALCULATIONS IN THE CORNELL ACCELERATOR-DESIGN SOFTWARE BMAD

Beam-breakup instabilities arising from higher-order-mode (HOM) power induced in the linac RF cavities have been modeled using Bmad tracking calculations by choosing an initial beam current with all RF buckets filled, tracking an off-axis beam to load HOM power, then testing for the time dependence of the highest HOM amplitude over a predetermined number of turns. A binary search for the threshold current then provides the instability limit to any chosen accuracy.

Solutions for the threshold current can be accurately approximated by simple formulas for the case of a single HOM in a single cavity where the HOM decay time is short or long relative to the return time [5]. Figure 2 shows the comparison of the Bmad tracking calculation to the analytic approximation of the threshold current for the toy model described in Ref. [5]. The HOM parameters are $R/Q = 100 \ \Omega$, $f_\lambda = 2.0$ GHz, and $Q_\lambda = 10^4$. For the purposes of validating the model, the return time to the cavity was scanned through the period of the BBU sensitivity determined by the HOM parameters and the bunch spacing. The result for the threshold current as a function of the ratio of the return time t_r to the time between bunches t_b (0.77 ns for the 1.3 GHz cavities) is compared to the analytic approximation.

Having demonstrated the accuracy of the BBU thresholds in the short-return-time limit, we apply the model to the full Cornell ERL optics with the same single HOM parameters modeled in a single cavity. This case exemplifies the limit of return times much greater than the HOM decay time. Figure 3 shows the result of the scan, demonstrating that the Bmad tracking reproduces the analytic approximation. The higher order mode parameters employed for this study are those of the first HOM of Ref. [6]: $R/Q = 71 \ \Omega$, $f_\lambda = 1.861$ GHz, and $Q_\lambda = 4968$.

EFFECTS OF LONGITUDINAL AND TRANSVERSE RESISTIVE-WALL WAKEFIELDS ON ERLS

N. Nakamura[#]

Institute for Solid State Physics(ISSP), University of Tokyo

5-1-5 Kashiwanoha, Kashiwa, Chiba 277-8581, Japan.

Abstract

Exact expressions of longitudinal and transverse resistive-wall impedances for a round pipe with a finite thickness were analytically obtained to accurately evaluate effects of resistive-wall wakefields on energy recovery linacs(ERLs). Parasitic loss in an ERL vacuum chamber due to the longitudinal impedance was evaluated and found to be serious compared with 3rd generation SR sources because of the shorter bunch length. It was also shown by the calculation result of longitudinal resistive-wall impedance of a two-layer round pipe that copper coating is effective for reducing the parasitic loss of a stainless steel(SS) chamber. Transverse resistive-wall wake functions of round pipes were numerically calculated using the exact impedance expression to simulate transverse multi-bunch beam motions due to resistive-wall wakefields in ERLs. Possibility of resistive-wall beam breakup(BBU) in the compact ERL and in a long undulator chamber of a 5-GeV ERL was discussed based on simulation results.

INTRODUCTION

In ERL-based synchrotron radiation(SR) sources, high-current and short-bunch beams are circulated. Such a beam can generate strong wakefields in resistive-wall ERL components and the wakefields seriously affect the components and the beam itself. Transverse multi-bunch beam breakup due to the resistive-wall wake was already studied with analytical and simulation approaches using the conventional expression of the resistive-wall wake function[1][2]. Although the study results implied that the beam position displacement due to the resistive-wall wake infinitely increases with time, it was also pointed out that the conventional expression of the resistive-wall wake function is valid only in a limited time range[2]. In this paper, exact expressions of the longitudinal and transverse impedances are derived to correctly estimate the resistive-wall impedances and their effects on ERLs. Transverse multi-bunch beam motions are simulated with the exact wake functions. Furthermore parasitic loss in a vacuum chamber due to the longitudinal resistive-wall wakefields is also evaluated.

EXACT EXPRESSIONS FOR RESISTIVE-WALL IMPEDANCES

Longitudinal Impedance

An exact expression of the longitudinal resistive-wall impedance (per unit length) of a round pipe with an inner radius b and a thickness d was analytically derived as follows:

$$Z_{//}(\omega) = \frac{-i}{2\pi\varepsilon_0 bc\left\{\left(\dfrac{\omega}{\lambda c} + \dfrac{\lambda c}{\omega}\right)\alpha_l - \dfrac{b\omega}{2c}\right\}} \tag{1}$$

$$\alpha_l = \frac{J_1(\lambda b)N_0(\lambda(b+d)) - N_1(\lambda b)J_0(\lambda(b+d))}{J_0(\lambda b)N_0(\lambda(b+d)) - N_0(\lambda b)J_0(\lambda(b+d))}$$

$$\lambda = \frac{i + sgn(\omega)}{\delta} \quad \left(\delta = \sqrt{\frac{2}{\sigma\mu_0|\omega|}}\right)$$

Here σ, ε_0, μ_0, c, i, ω, and δ are the electric conductivity of the pipe, the permittivity and permeability of vacuum, the velocity of light, the imaginary unit, the angular frequency and the skin depth of the pipe, and J_0, J_1, N_0 and N_1 are the 0th-order and 1st-order Bessel functions of the 1st and 2nd kinds, respectively. The permittivity and permeability of the pipe are assumed to be equal to or approximated by those of vacuum. The $sgn(\omega)$ means the sign of ω. If the pipe thickness becomes infinity, the expression is rewritten as Eq. (2) with the 0th-order and 1st-order Hankel functions of the 1st kind, $H_0^{(1)}$ and $H_1^{(1)}$.

$$Z_{//}(\omega) = \frac{-i}{2\pi\varepsilon_0 bc\left\{\left(\dfrac{\omega}{\lambda c} + \dfrac{\lambda c}{\omega}\right)\dfrac{H_1^{(1)}(\lambda b)}{H_0^{(1)}(\lambda b)} - \dfrac{b\omega}{2c}\right\}} \tag{2}$$

If one considers the frequency range satisfying the conditions of $|\lambda|b \gg 1$, $|\lambda| \gg |\omega/c|$, $|\lambda| \gg b\omega^2/c^2$, the conventional impedance expression of Eq. (3) is derived from Eq. (2).

$$Z_{//}(\omega) = \frac{\omega Z_0 \delta}{4\pi bc}\{sgn(\omega) - i\} \quad \left(Z_0 = \sqrt{\frac{\mu_0}{\varepsilon_0}}\right) \tag{3}$$

Here Z_0 is the impedance of vacuum.

Figure 1 shows the real parts of the resistive-wall impedances of stainless steel(SS) pipes with b=8 mm and σ=1.4×10⁶ Ω⁻¹m⁻¹ calculated from Eqs. (1) and (2). For comparison, the conventional expression of Eq. (3) is shown in the figure. The real parts of the exact impedances have two kinds of cut-offs, low and high frequency cut-offs. The high-frequency cut-off depends on only the pipe radius. On the other hand, the low-frequency cut-off depends on both pipe radius and thickness. Only in the intermediate frequency range, the impedances are approximated by Eq. (3) as shown in Fig. 1.

[#]nakamura@issp.u-tokyo.ac.jp

Optics & Beam Dynamics